

doi:10.3799/dqkx.2016.128

东准噶尔晚石炭世双峰式火山岩年代学、地球化学及其构造意义

罗婷^{1,2}, 陈帅³, 廖群安², 陈继平¹, 胡朝斌⁴, 王富明⁵, 田健⁶, 吴魏伟⁷

1. 陕西省地质调查中心, 陕西西安 710054

2. 中国地质大学地球科学学院, 湖北武汉 430074

3. 中国冶金地质总局西北局, 陕西西安 710054

4. 中国地质调查局西安地质调查中心, 陕西西安 710054

5. 四川省地质矿产勘查开发局四〇五地质队, 四川都江堰 611830

6. 中国地质调查局天津地质调查中心, 天津 300170

7. 中国地质科学院地质研究所大陆构造与动力学国家重点实验室地幔研究中心, 北京 100037

摘要:新疆东准噶尔卡拉麦里造山带晚石炭世双峰式火山岩很好地记录了中亚造山带晚古生代时期洋陆转换阶段复杂的岩浆作用过程, 对该过程的详细剖析能更好地理解中亚造山带的地质历史。通过该区域晚石炭世巴塔玛依内山组火山岩详细的岩石学、地球化学、锆石 U-Pb 年代学和 Sr-Nd-Pb 同位素组成的研究, 并结合区域上已有的研究成果, 获得了如下认识: (1) 该套火山岩组合形成于晚石炭世早期 320.2 ± 4.2 Ma, 为晚石炭世早期陆相喷发的产物。火山岩具明显的双峰式组合的特征, 基性端元由碱性系列和拉斑系列的玄武岩、玄武质粗面安山岩组成; 酸性端元由粗面岩和流纹岩组成, 成分上相当于 A 型花岗岩; (2) 岩石地球化学和同位素特征显示, 该套双峰式火山岩来源于不同的岩浆源区, 基性岩来自于亏损的地幔源区, 在岩浆上升过程中发生橄榄石及单斜辉石的分离结晶作用并遭受了地壳混染, 而酸性岩来自于下地壳的部分熔融; (3) 该套双峰式火山岩产出于后碰撞末期的构造环境, 由于洋壳的拆沉作用而引发软流圈上涌, 使得上覆的地幔发生部分熔融产生岩浆, 同时由于底侵作用导致地壳下部发生部分熔融, 喷发出地表形成该双峰式火山岩套, 这套双峰式火山岩的出现, 标志着东准噶尔卡拉麦里地区造山作用进入尾声。

关键词: 双峰式火山岩; 晚石炭世; 后碰撞末期; 东准噶尔; 地球化学; 岩石学。

中图分类号: P581

文章编号: 1000-2383(2016)11-1845-18

收稿日期: 2016-03-10

Geochronology, Geochemistry and Geological Significance of the Late Carboniferous Bimodal Volcanic Rocks in the Eastern Junggar

Luo Ting^{1,2}, Chen Shuai³, Liao Qun'an², Chen Jiping¹, Hu Chaobin⁴, Wang Fuming⁵, Tian Jian⁶, Wu Weiwei⁷

1. Shanxi Geological Survey Center, Xi'an 710054, China

2. Faculty of Earth Sciences, China University of Geosciences, Wuhan 430074, China

3. Northwest Bureau of China Metallurgical Geology, Xi'an 710054, China

4. Xi'an Center of Geological Survey, China Geological Survey, Xi'an 710054, China

5. No.405 Geological Party, Sichuan Bureau of Geology and Mineral Exploration and Development, Dujiangyan 611830, China

6. Tianjin Center of Geological Survey, China Geological Survey, Tianjin 300170, China

7. CARMA, State Key Laboratory for Continental Tectonics and Dynamics, Institute of Geology, Chinese Academy of Geological Sciences, Beijing 100037, China

Abstract: The study region locates in the southwest margin of Central Asian Orogenic belt, which recorded several volcanic events of

基金项目: 中国地质调查局计划项目(No.12120114042801)。

作者简介: 罗婷(1987-), 女, 博士, 从事岩浆岩及其相关矿产研究工作。E-mail: 179175768@qq.com

引用格式: 罗婷, 陈帅, 廖群安, 等, 2016. 东准噶尔晚石炭世双峰式火山岩年代学、地球化学及其构造意义. 地球科学, 41(11): 1845-1862.

different tectonic environment. The volcanic rocks from Late Carboniferous Batamayineishan Formation includes the alkaline series and sub-alkaline series, which formed in 320.2 ± 4.2 Ma. They have a SiO_2 interrupt ranging from 56% to 67.5%. The basaltic rocks and the felsic rocks are closely associated. They show a typical characteristic of bimodal volcanic rocks. Their geochemistry and isotope characteristics suggesting that the basaltic rocks come from a depleted mantle source whereas the felsic rocks come from a source due to anatexic melting of the lower crust and show characteristic of A-type granites. The assemblages of volcanic rocks and the geochemical information of volcanic rocks from Batamayineishan Formation indicate they formed in apost-collision environment. Combining the research results of this region, the authors consider the Batamayineishan Formation were generated mainly in the end stage of post-collision of Kalamaili orogenic, which began after cessation of collision, and involved extensional detachment of the thickened lithosphere, leading to extension and thinning of the crust.

Key words: bimodal volcanic rocks; Late Carboniferous; post-collision; eastern Jungar; geochemistry; petrology.

0 引言

中亚造山带西南部的东准噶尔造山带卡拉麦里地区发育了大量的晚石炭世火山岩,该套火山岩的形成背景一直存在较大争议,主要有以下 4 种观点:(1)该套火山岩是大洋俯冲消减阶段产生的岛弧火山岩(Xiao, 2008; Geng *et al.*, 2009);(2)它形成于不成熟的弧后盆地;(3)该套火山岩是后碰撞阶段的产物(韩宝福, 2006; 王京彬和徐新, 2006; 吴润江等, 2009; 李涤等, 2012);(4)它是板内裂谷环境下的产物(李锦轶等, 1990; 朱志新等, 2005).除此之外,学者们对于该组火山岩的形成时代也有争议,张元元等(2009)在卡拉麦里断裂带北侧扎河坝地区流纹岩中获得锆石加权平均年龄为 275.6 ± 2.8 Ma, 将其划归为二叠纪;谭佳奕等(2009)对卡拉麦里南侧的粗面安山岩定年,获得锆石年龄为 350.0 ± 6.3 Ma, 将该地层归入下石炭统;苏玉平等(2010)对卡拉麦里白碱沟钻井中的玄武岩锆石定年,获得锆石年龄为 300.4 ± 1.3 Ma, 认为该地层应归入晚石炭世末期.笔者通过对该套火山岩详细的实测剖面研究,认为其是晚石炭世(320 Ma)发育的一套典型的双峰式火山岩组合.事实上,笔者通过野外调查发现,该套火山岩确为基性端元与酸性端元互层的典型双峰式火山岩,缺少中性端元;而谭佳奕等(2009)定年所采粗面安山岩可能属于其采样剖面附近的早石炭世松喀尔苏组火山岩,该组火山岩出现类似的岩性.张元元等(2009)所测锆石的岩石来自扎河坝地区,该区大量发育早二叠世或更晚的基性岩脉,苏玉平等(2010)认为广泛的基性岩浆作用可能对这些岩石中的锆石有重置作用.

通常认为,双峰式火山岩与伸展构造作用有关,但双峰式火山岩形成的地球动力学环境存在多样性,近年来的研究发现,双峰式火山岩不仅可以产于

大陆裂谷环境,在地球动力学特征明显不同的环境也有产出,如后碰撞造山(Frisch *et al.*, 2000)、弧后盆地、活动大陆边缘(Donnelly and Rogers, 1980)、洋内岛弧(Geist, 1995)等.另外,对于双峰式火山岩中的酸性端元的成因也有两种截然不同的成因机制被提出:(1)与玄武质岩石同源区,由玄武质岩浆演化而来(Turner *et al.*, 1992; Mungall and Martin, 1995; Civetta *et al.*, 1998; Ngounounoa *et al.*, 2000; Shinjo and Kato, 2000; Peccerillo *et al.*, 2003; Tian *et al.*, 2010);(2)由来自于底侵岩浆诱发的下地壳深熔作用(Davies and Macdonald, 1987; Sage *et al.*, 1996; Trua *et al.*, 1998; Pamić *et al.*, 2000; Wareham *et al.*, 2001; van Wagoner *et al.*, 2002; Brewer *et al.*, 2004).

前人对该组火山岩的喷发时间、形成环境有多种不同的认识,探讨该双峰式火山岩的成因意义、形成机制和产出环境,对新疆北部古生代洋陆演化具有重要的约束意义,同时可为恢复造山带大地构造格局提供有力证据.本文通过对火山岩的 LA-ICP-MS 锆石 U-Pb 年代学,全岩主微量元素及 Sr-Nd 同位素地球化学特征研究,认为该套火山岩形成于晚石炭世,是后碰撞末期的岩浆活动产物.对东准噶尔造山带卡拉麦里地区晚石炭世双峰式火山岩的研究,将有助于人们更好地理解中亚造山带西南部晚石炭世时的构造演化及深部动力学过程.

1 区域地质概况及火山地质特征

中亚造山带是世界上最大的造山带,是大洋开启与俯冲、板块碰撞拼合、后造山造山运动不同阶段演化的结果.它北邻西伯利亚克拉通,南倚华北克拉通和塔里木克拉通(图 1a),由岛弧、蛇绿岩、洋岛、海山、增生楔、洋底高原和微陆块等增生拼贴而成.

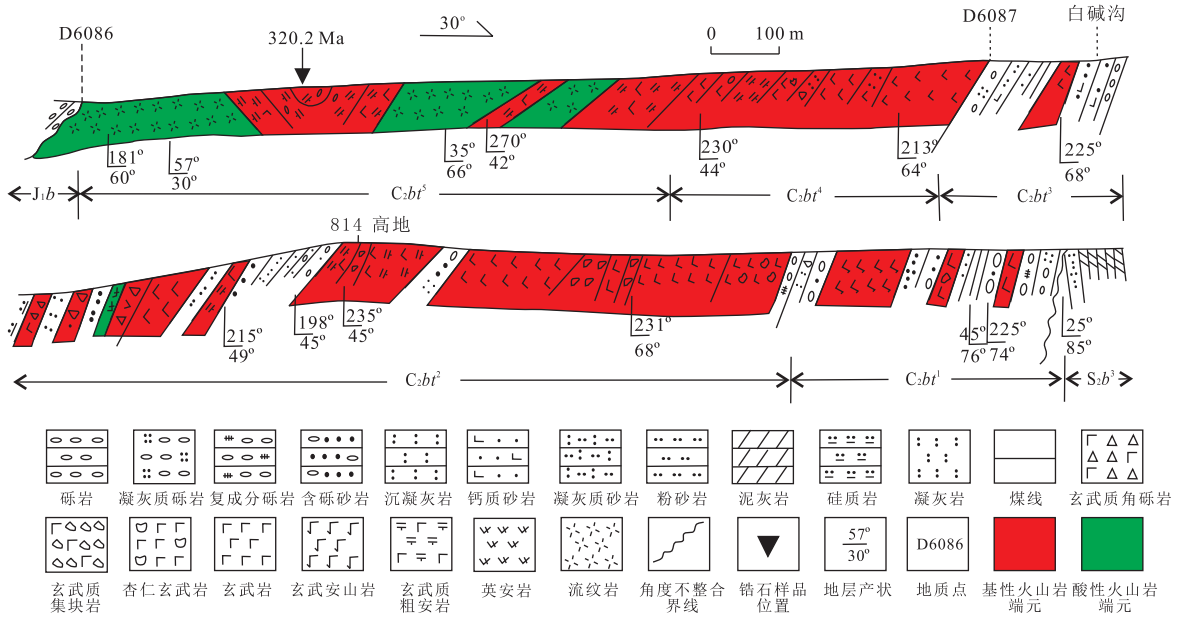


图 2 东准噶尔卡拉麦里地区晚石炭世巴塔玛依内山组典型地质实剖面

Fig.2 The typical geological sections for volcanic rocks from the Late Carboniferous Batamayineishan Formation, eastern Junggar

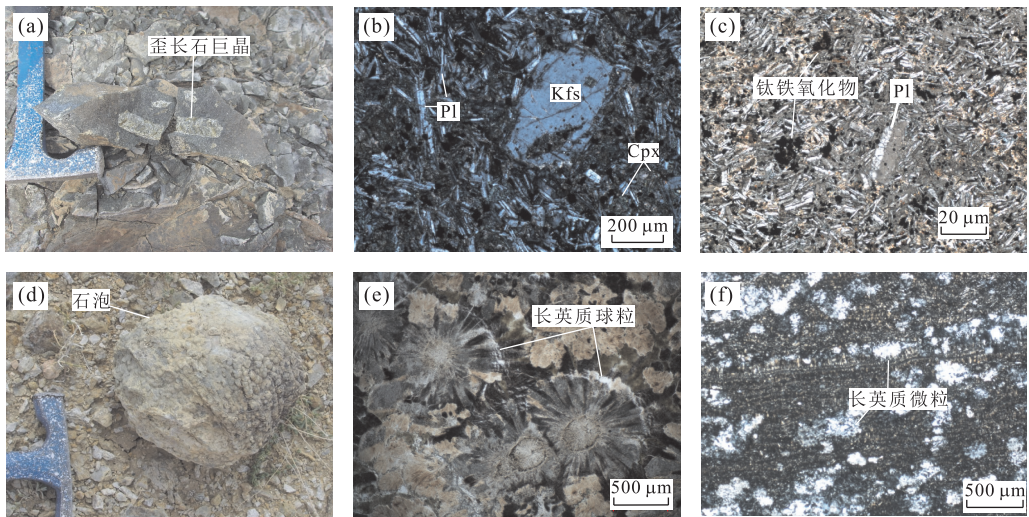


图 3 东准噶尔卡拉麦里地区晚石炭世巴塔玛依内山组双峰式火山岩火山岩野外照片(a,d)和显微照片(b,c,e,f)

Fig.3 Field photos (a,d) and Photomicrographs (b,c,e,f;cross-polarized light) of volcanic rocks from Late Carboniferous Batamayineishan Formation, eastern Junggar

a.碱性玄武岩及歪长石斑晶;b.碱性玄武岩碱性长石斑晶;c.拉斑玄武岩斜长石斑晶和钛铁氧化为微粒;d.流纹岩石泡构造;e.流纹岩基质球粒结构;f.流纹岩流纹构造;Pl.斜长石;Kfs.钾长石;Cpx.单斜辉石

合为钙质砾岩、砂岩、长石砂岩、炭质泥岩与玄武岩及火山角砾岩互层,火山活动以间歇式的中基性熔岩的溢流为特点,由多个沉积—溢流韵律组成,喷发间歇期的沉积岩厚度大,主要为钙质砾岩、砂岩和炭质粉砂—泥岩,含多条煤线,但煤层厚度较小.该亚旋回是巴塔玛依内山组中火山活动相对平静的阶段.

第 4 亚旋回 (C_{2bt}^4): 该亚旋回与第 2 旋回相似,岩性组合为巨厚的玄武质熔岩,夹少量的安山

质、流纹质凝灰岩和凝灰质砂岩.以巨厚连续多层的溢流式喷发为特征,韵律性不明显,但该亚旋回下部主要为巨厚层的玄武岩,上部主要为玄武粗安岩,从下向上具明显的由基性向中基性演化的规律.

第 5 亚旋回 (C_{2bt}^5): 由流纹岩、粗面岩和玄武岩互层组成,以出现大量的流纹岩、粗面岩、珍珠岩及相应的火山碎屑岩为特征.由多个玄武岩—流纹岩的韵律组成.

该套火山岩中基性熔岩发育有很好的顶底构造,顶部的氧化带常具紫红色,气孔带发育,中部多为无气孔的块状构造,其结晶程度明显好于顶底,底部呈灰绿色—深灰色,在碱性玄武岩中见歪长石巨晶(图 3a)。酸性流纹质熔岩常与侵出相的流纹斑岩伴生,在侵出相流纹斑岩附近常有玻璃质流纹岩(珍珠岩)产出,是近火口相的标志。

2 岩相学特征

(碱性)玄武岩、粗面玄武岩:灰绿色—灰黑色,斑状结构,基质具间粒间隐结构,杏仁状、块状构造,在碱性玄武岩中见歪长石巨晶(图 3a,3b)。斑晶由普通辉石(10%)和斜长石组成,偶见已伊丁石化的橄榄石。斜长石斑晶部分见环带结构,粒径可达 1 mm。基质由微晶斜长石($An=67$)和辉石组成,含少量的磁铁矿。区内出露的拉班玄武岩镜下可见大量的钛铁氧化物颗粒(图 3c)。

玄武粗安岩:灰色—灰绿色,斑状结构,块状、气孔构造,大部分岩石基质为玻基交织结构。斑晶斜长石(5%~10%)、辉石,极少量岩石中见角闪石斑晶(具暗化边)。部分岩石中可见有少量橄榄石斑晶。基质中斜长石微晶多属中长石,辉石微晶、玻璃质及磁铁矿充填在微晶斜长石粒间。

粗面岩:灰色—灰褐色,斑状结构,基质具粗面结构。斑晶为钾长石(15%),呈板柱状自形晶产出,发育卡氏双晶。基质主要由板柱状的碱性长石微晶组成,含少量的针状斜长石微晶,微晶长石呈半定向分布,粒间被火山玻璃质及少量的辉石微粒、磁铁矿充填。

流纹岩:岩石新鲜断口呈肉红色、红棕色(珍珠岩),斑状结构,基质为霏细结构、球粒结构和玻璃质结构(珍珠岩),流纹构造,珍珠岩中伴有珍珠构造。熔岩层中上部常见流纹构造、石泡构造(图 3d~3f)。斑晶由透长石、石英和少量的黑云母组成,黑云母呈褐色—红褐色,常具暗化边结构。基质主要由霏细状、球粒状的长英质矿物组成,含少量火山玻璃和磁铁矿。

3 样品与分析方法

3.1 锆石 U-Pb 测年

本文在野外路线调查和剖面测制基础上共采集了 2 件锆石 U-Pb 同位素测年样品,岩性分别为玄武粗安岩和流纹斑岩。测年样品的粉碎加工、分离、挑选

工作由河北省廊坊市诚信地质服务有限公司完成。锆石制靶、透反射光和阴极发光(cathode luminescence, CL)显微照相在中国地质大学(武汉)地质过程与矿产资源国家重点实验室完成。锆石 LA-ICP-MS 测试也在在中国地质大学(武汉)地质过程与矿产资源国家重点实验室进行。用于分析测试的锆石颗粒无包体、无裂纹、岩浆环带清楚;用于测试的激光剥蚀系统为 GeoLas 2005, ICP-MS 为 Agilent 7500a, 激光斑束直径为 32 μm 。样品分析流程:在开始测量和测定结束后分别测定 Nist610、91500、GJ-1 标样,每隔 5 个分析点测定 2 次锆石标样 91500。测试结果由 ICPMSDataCal 软件处理。详细的处理流程和数据的处理方法见相关文献(Liu *et al.*, 2008)。样品的锆石 U-Pb 同位素年龄谱和图的绘制和年龄权重平均计算均采用 Isoplot 3.0 (Ludwig, 2003)完成。

3.2 主微量元素

在野外实测剖面 and 路线地质调查基础上,笔者选择了较新鲜、气孔和杏仁体较少的样品进行测试。对于一些有杏仁体的样品,先在颚式刚玉对滚机上将其粉碎到厘米级大小,剔除含杏仁的部分,部分含细小方解石的样品用盐酸浸泡后再清洗干净后,用于分析。全岩主量元素、微量及稀土元素分析测试的样品共 30 件,分析测试由湖北省地质实验研究所完成。主量元素用 X 射线荧光光谱仪测定,分析精度(relative standard deviation, RSD)小于 0.9% (除 H_2O 、 CO_2)。微量及稀土元素由电感耦合等离子质谱仪(ICP-MS)测定。

3.3 Sr-Nd-Pb 同位素

Sr-Nd-Pb 同位素测试的样品共 11 件, Sr-Nd 同位素样品测试工作在中国地质大学(武汉)国家重点实验室完成,采用 Finnigan 公司的 MAT261 进行比值测量,准确度通过标样 NBS987 和 La Jolla 国际标样进行监测, Sr 同位素的质量分馏用 $^{86}\text{Sr}/^{88}\text{Sr} = 0.1194$ 校正, Nd 同位素质量分馏用 $^{146}\text{Nd}/^{144}\text{Nd} = 0.7219$ 校正, Pb 同位素的分离和测试均在西北大学大陆动力学国家重点实验室完成。应用高分辨多接收等离子体质谱仪(Nu Plasma HR)测试,在测定样品之前,用 NBS981 标准校定仪器,测试过程中采用 NBS997-T1 作为内标进行质量分馏校正,随时测定 NBS981 来监测仪器,样品的测定条件同 NBS981 相同。在标准测试程序的基础上所有 Pb 同位素分析的精度在 95% 置信度下优于 0.05%。

4 结果

4.1 锆石 U-Pb 测年

笔者选送了该套地层中的玄武粗面岩样品、流纹岩样品和后期侵入该组流纹岩地层的流纹斑岩进行 LA-ICP-MS 锆石 U-Pb 定年。流纹岩样品所挑选锆石小而少,测试结果不理想,采集位置见图 1c,玄武粗面岩样品和流纹斑岩样品的锆石分析结果见表 1。玄武

粗面岩锆石颗粒半自形—自形,呈浅黄色、无色,透明—半透明的正方双锥状、柱状及锥状自形晶体,具有明显的岩浆震荡环带(图 4)。流纹斑岩锆石基本具有自形、透明特点,且具有较大的长宽比,显示为酸性岩结晶锆石特点。笔者选择无色透明、晶形较好的锆石进行测试。选择测试的锆石 Th/U 值为 0.41~0.97(表 1),显示为岩浆锆石的特点(Vavra *et al.*, 1999),玄武粗面岩锆石样品加权平均年龄结果为

表 1 东准卡拉麦里地区粗面岩(008-15)及流纹斑岩(056-5)锆石 U-Pb 同位素分析

Table 1 Analysis results of zircon U-Pb age from the volcanic rocks from Late Carboniferous Batamayineishan Formation

分析号	Pb (10^{-6})	Th (10^{-6})	U (10^{-6})	Th/U	$^{207}\text{Pb}/^{206}\text{Pb}$	1σ	$^{207}\text{Pb}/^{235}\text{U}$	1σ	$^{206}\text{Pb}/^{238}\text{U}$	1σ	年龄(Ma)		谐和度(%)
											$^{206}\text{Pb}/^{238}\text{U}$	1σ	
008-15-01	77.50	523.84	627.56	0.83	0.056 7	0.002 9	0.387 4	0.019 8	0.049 8	0.000 7	313	5	94
008-15-04	55.97	248.55	404.88	0.61	0.072 3	0.003 6	0.527 5	0.025 9	0.053 8	0.000 9	338	5	75
008-15-05	56.88	313.75	501.29	0.63	0.064 0	0.003 6	0.452 2	0.025 8	0.051 6	0.000 7	324	4	84
008-15-07	59.59	331.23	471.80	0.70	0.067 7	0.002 9	0.489 9	0.022 1	0.052 7	0.000 9	331	5	80
008-15-09	66.93	391.50	568.74	0.69	0.053 3	0.002 6	0.377 3	0.018 4	0.052 0	0.000 8	327	5	99
008-15-10	50.59	272.93	467.88	0.58	0.065 0	0.003 2	0.443 8	0.021 4	0.050 4	0.000 8	317	5	83
008-15-12	47.76	279.99	470.04	0.60	0.051 7	0.002 9	0.344 6	0.018 5	0.049 4	0.000 7	311	4	96
008-15-13	45.28	219.78	448.15	0.49	0.059 5	0.003 6	0.422 6	0.024 1	0.052 7	0.000 8	331	5	89
008-15-15	53.08	286.30	473.99	0.60	0.058 0	0.002 9	0.413 5	0.022 0	0.051 3	0.000 7	322	5	91
008-15-16	61.01	325.89	534.84	0.61	0.058 8	0.003 6	0.415 2	0.026 7	0.051 0	0.000 8	320	5	90
008-15-17	57.52	277.21	478.41	0.58	0.062 5	0.003 0	0.472 0	0.022 1	0.054 9	0.000 8	344	5	86
008-15-19	70.24	402.97	615.56	0.65	0.057 2	0.002 9	0.407 6	0.020 9	0.051 5	0.000 7	324	4	92
008-15-20	58.34	344.04	541.75	0.64	0.053 3	0.002 5	0.373 2	0.017 7	0.051 0	0.000 8	321	5	99
008-15-21	81.44	314.65	515.80	0.61	0.099 1	0.007 6	0.794 0	0.077 9	0.054 3	0.001 1	341	7	45
008-15-22	63.83	354.64	478.92	0.74	0.058 5	0.003 0	0.434 7	0.022 5	0.054 6	0.000 8	343	5	89
008-15-23	123.03	767.30	791.64	0.97	0.051 1	0.002 5	0.365 0	0.016 9	0.052 1	0.000 7	327	4	96
008-15-24	70.90	372.11	613.15	0.61	0.054 2	0.002 7	0.384 9	0.019 7	0.051 3	0.000 7	323	4	97
008-15-25	39.19	207.95	369.18	0.56	0.054 9	0.003 4	0.396 5	0.024 5	0.052 1	0.000 8	327	5	96
056-5-1-01	6.88	58.09	121.76	0.48	0.056 3	0.003 5	0.379 7	0.022 2	0.049 3	0.000 7	310	4	94
056-5-1-02	5.73	48.47	99.76	0.49	0.058 3	0.003 5	0.398 5	0.023 9	0.050 1	0.000 8	315	5	92
056-5-1-03	8.62	86.65	148.57	0.58	0.053 4	0.003 1	0.361 8	0.021 1	0.049 5	0.000 8	311	5	99
056-5-1-04	9.29	87.91	164.37	0.53	0.055 0	0.002 7	0.365 4	0.018 2	0.047 9	0.000 7	302	4	95
056-5-1-05	7.43	67.58	131.48	0.51	0.056 9	0.003 8	0.371 2	0.020 3	0.048 8	0.000 8	307	5	95
056-5-1-06	10.01	103.89	151.70	0.68	0.073 4	0.004 2	0.521 7	0.029 5	0.051 5	0.000 9	324	5	72
056-5-1-07	14.20	197.65	221.96	0.89	0.056 9	0.002 3	0.387 8	0.014 8	0.049 3	0.000 7	310	4	93
056-5-1-08	7.65	83.64	133.57	0.63	0.055 0	0.003 0	0.363 5	0.020 7	0.047 8	0.000 8	301	5	95
056-5-1-09	16.15	239.69	261.80	0.92	0.053 0	0.002 3	0.351 9	0.015 7	0.047 6	0.000 6	300	4	97
056-5-1-11	13.28	132.84	218.82	0.61	0.064 2	0.003 2	0.447 0	0.023 4	0.049 5	0.000 7	311	4	81
056-5-1-12	7.89	69.50	129.09	0.54	0.060 1	0.004 3	0.429 9	0.031 1	0.052 1	0.000 9	327	6	89
056-5-1-13	9.22	103.47	155.38	0.67	0.055 2	0.003 3	0.371 4	0.021 1	0.048 5	0.000 8	305	5	95
056-5-1-16	10.29	103.71	178.21	0.58	0.053 5	0.002 1	0.361 6	0.014 4	0.048 6	0.000 7	306	4	97
056-5-1-17	7.50	62.58	131.81	0.47	0.053 8	0.003 2	0.371 8	0.021 0	0.050 3	0.000 8	316	5	98
056-5-1-18	9.56	117.22	151.51	0.77	0.053 1	0.002 8	0.358 8	0.017 2	0.050 6	0.000 9	318	6	97
056-5-1-19	7.59	82.02	132.14	0.62	0.053 3	0.003 1	0.353 2	0.019 9	0.048 8	0.000 8	307	5	99
056-5-1-20	8.53	87.84	141.99	0.62	0.052 1	0.002 8	0.362 7	0.019 8	0.050 4	0.000 7	317	4	99
056-5-1-21	9.69	106.91	161.13	0.66	0.054 4	0.002 9	0.372 7	0.019 3	0.050 5	0.000 8	318	5	98
056-5-1-22	6.44	52.75	108.69	0.49	0.072 9	0.004 7	0.485 8	0.030 6	0.049 2	0.000 8	310	5	74
056-5-1-24	5.56	44.85	97.32	0.46	0.055 9	0.002 9	0.371 0	0.018 5	0.049 0	0.000 9	308	5	96
056-5-1-26	11.38	127.88	185.60	0.69	0.056 9	0.002 6	0.375 4	0.016 6	0.048 8	0.000 7	307	4	94

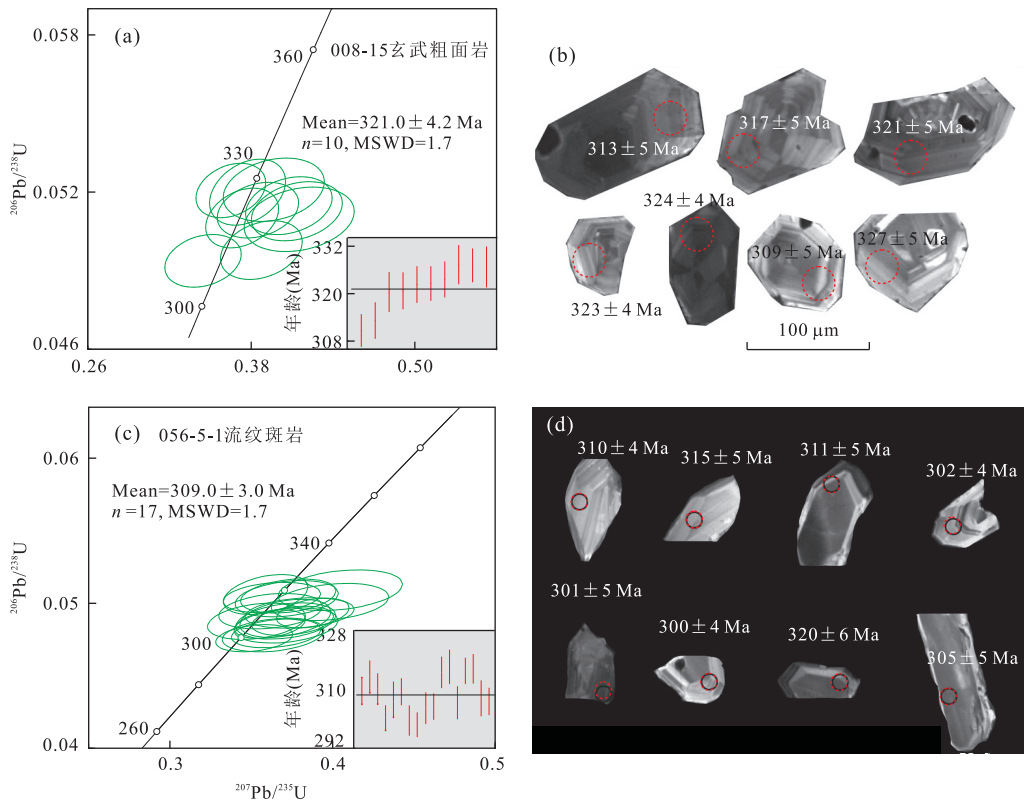


图 4 东准噶尔卡拉麦里地区巴塔玛依内山组双峰式火山岩锆石 LA-ICP-MS U-Pb 谐和年龄图(a,b)和锆石阴极发光照片(c,d)
Fig.4 LA-ICP-MS zircon U-Pb age concordia diagrams, weighted mean ages (a,b) and representative CL images (c,d) of zircons from the volcanic rocks from Late Carboniferous Batamayineishan Formation, eastern Junggar

321.0 ± 4.2 Ma(图 4a),流纹斑岩锆石样品加权平均年龄结果为 309.1 ± 3.0 Ma(图 4b)。结果显示该组火山岩形成于 321.0 ± 4.2 Ma,为晚石炭世早期岩浆活动的产物,并在后期被 309.1 ± 3.0 Ma 的流纹斑岩侵入。流纹斑岩一般形成于火山喷发阶段的后期,它们是高粘度熔浆舌在流动过程中,从火山通道或附近裂隙中缓慢地以“挤牙膏式”挤出地表,堆积成的穹丘状地质体。研究区内见到的侵入相通常为深红色流纹构造流纹斑岩。根据野外关系及区域地质判断,该流纹斑岩可能为该区域火山活动末期所形成,并侵入到早期形成的流纹岩地层中。这与朱志新等(2005)在该地层中发现的晚石炭世化石结果一致。

4.2 主量及微量元素特征

全岩主微量元素分析结果见表 2。少量样品遭受了低温蚀变,与分析结果中的烧失量和岩相学特征一致。在图 5a 中,本文数据主要落在玄武岩区、玄武质粗面安山岩区和流纹岩区内, SiO_2 值为 $56.0\% \sim 67.5\%$ 时出现明显的间断,区域资料也显示出中性端元火山岩的缺失,证实该组火山岩具双峰式分布特征。

中基性岩样品位于 Ir-Irvine 分界线两侧,分属

碱性系列和拉斑系列(图 5a, 5b),显示富碱($\text{Na}_2\text{O} + \text{K}_2\text{O}$ 大部分在 $4.09\% \sim 6.35\%$),富 TiO_2 ($1.55\% \sim 3.10\%$),具有较低的 K_2O 含量(中钾和低钾, $\text{K}_2\text{O} + 2 < \text{Na}_2\text{O}$),属钠质类型(图 6)。 MgO 含量($1.34\% \sim 5.13\%$)及 $\text{Mg}^\#$ 值($20 \sim 49$)变化范围大,且明显低于幔源原生岩的 $\text{Mg}^\#$ 值(65),相容元素 Ni ($0.6 \times 10^{-6} \sim 92.4 \times 10^{-6}$)和 Cr ($1 \times 10^{-6} \sim 188 \times 10^{-6}$)含量较低,均低于原始岩浆的参考数值,反映经历了较强的镁铁矿物的分离结晶作用。球粒陨石标准化微量元素蛛网图显示该基性端元类似于大陆碱性玄武岩的特征,但 Nb 和 Ta 元素相对亏损(图 7a)。球粒陨石标准化稀土曲线具有右倾特征(图 7a),显示为轻稀土相对富集、重稀土相对亏损的分配模式, $(\text{La}/\text{Yb})_N$ 值为 $3.23 \sim 5.21$ 。

酸性岩样品中 SiO_2 含量较高且变化大,为 $67.5\% \sim 76.9\%$;随 SiO_2 含量增加,TFeO、MnO 含量基本上逐渐减少;岩石具有富 Al_2O_3 ($11.70\% \sim 15.25\%$)、 Na_2O ($3.13\% \sim 4.49\%$)、 K_2O ($2.77\% \sim 5.91\%$)、贫 MgO ($0.04\% \sim 0.31\%$)、 CaO ($0.11\% \sim 0.73\%$)、TFeO ($0.77\% \sim 4.77\%$)的特征,这与东准

表 2 巴塔玛依内山组火山岩主量元素(%)和微量元素(10⁻⁶)分析结果
Table 2 Analysis results of major elements (%) and trace elements (10⁻⁶) from the volcanic rocks of Late Carboniferous Batamayneishan Formation

Table with columns for sample ID (e.g., 008-7, 008-8) and chemical elements (e.g., SiO2, TiO2, Al2O3, Fe2O3, FeO, MnO, MgO, CaO, Na2O, K2O, P2O5, LOI, Total, Ce, Pr, Nd, Sm, Eu, Gd, Tb, Dy, Ho, Er, Tm, Yb, Lu, ΣREE, Eu*/Eu*, (La/Yb)N, (La/Sm)N, (Gd/Yb)N, Cr, Ni, Co, Rb, Cs, Sr, Ba, V, Sc, Nb, Ta, Zr, Hf, U, Th, Pb, Y). The table is divided into sections for major elements and trace elements, with sub-sections for acid rocks and mafic rocks.

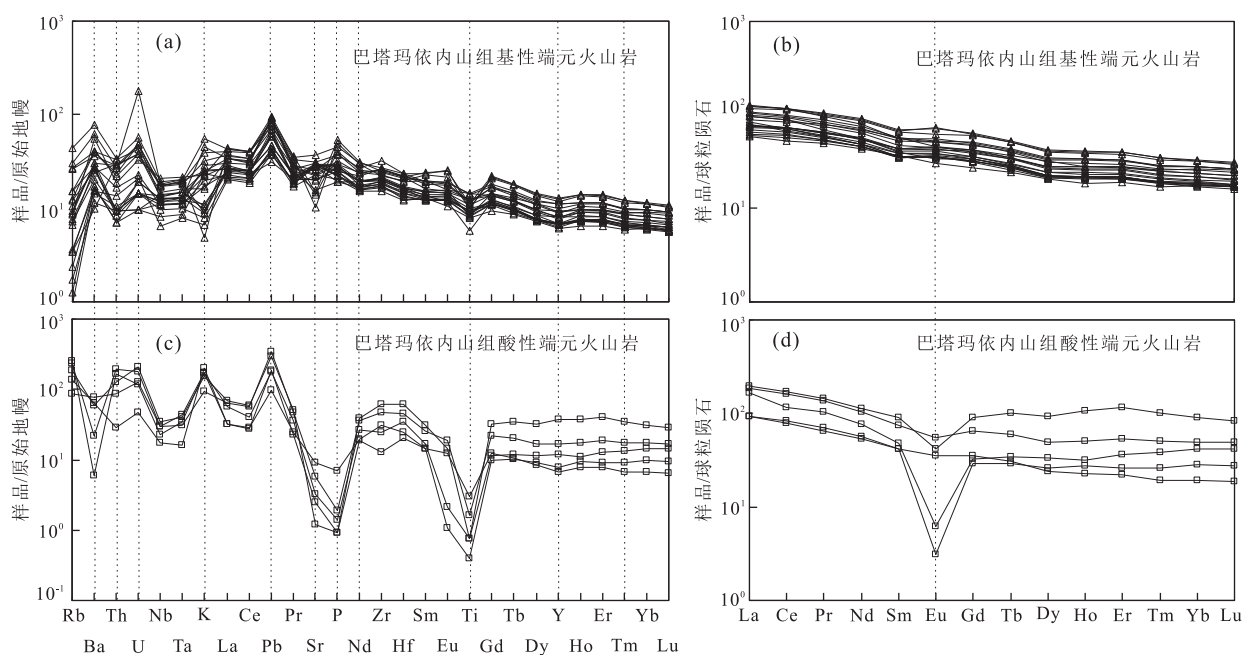


图 7 东准噶尔卡拉麦里地区巴塔玛依内山组双峰式火山岩微量元素标准化蛛网图(a,c)和稀土元素球粒陨石标准化型式(b,d)

Fig.7 Primitive mantle normalized multi-element patterns (a,c) and chondrite-normalized rare earth element (REE) patterns (b,d) of the volcanic rocks from Late Carboniferous Batamayineishan Formation, eastern Junggar

标准化值据 Sun and McDonough(1989)

表 3 巴塔玛依内山组火山岩 Sr、Nd、Pb 同位素数据

Table 3 Analysis results of Sr-Nd-Pb isotopes from the volcanic rocks of Late Carboniferous Batamayineishan Formation

样品	玄武岩					流纹岩			
	008-9	008-17	008-25	008-35	008-37	008-75	008-85	060-59	060-85
$T(\text{Ma})$	320/巴塔玛依内山组								
$^{87}\text{Rb}/^{86}\text{Sr}$	0.034 622	0.192 715	0.206 164	0.004 235	0.031 906	0.020 825	0.058 646	8.896 372	6.300 169
$^{87}\text{Sr}/^{86}\text{Sr}$	0.705 644	0.704 772	0.705 982	0.703 593	0.703 420	0.703 555	0.704 254	0.747 910	0.738 425
$(^{87}\text{Sr}/^{86}\text{Sr})_i$	0.705 486	0.703 894	0.705 043	0.703 574	0.703 275	0.703 460	0.703 987	0.707 393	0.709 732
$(^{87}\text{Sr}/^{86}\text{Sr})_{\text{CHUR}(t)}$	0.704 123	0.704 123	0.704 123	0.704 123	0.704 123	0.704 123	0.704 123	0.704 123	0.704 123
$^{147}\text{Sm}/^{144}\text{Nd}$	0.155 505	0.150 797	0.153 102	0.153 764	0.157 101	0.147 769	0.153 281	0.154 838	0.125 959
$^{143}\text{Nd}/^{144}\text{Nd}$	0.512 869	0.512 850	0.512 779	0.512 796	0.512 907	0.512 866	0.512 873	0.512 852	0.512 827
$\epsilon_{\text{Nd}}(t)$	6.194 582	6.016 204	4.535 855	4.840 648	6.871 176	6.452 420	6.363 665	5.896 829	6.588 943
$T_{\text{DM1}}\text{Nd}(\text{Ga})$	0.736 544	0.727 514	0.933 274	0.900 447	0.655 073	0.657 231	0.699 409	0.771 252	0.561 331
$T_{\text{DM2}}\text{Nd}(\text{Ga})$	0.573 208	0.587 788	0.708 216	0.683 415	0.518 090	0.552 286	0.559 465	0.597 457	0.541 290
$(^{206}\text{Pb}/^{204}\text{Pb})_i$	17.87 255	17.953 01	18.005 13	18.071 10	17.825 96	17.812 44	17.910 67	18.022 33	17.866 80
$(^{207}\text{Pb}/^{204}\text{Pb})_i$	15.50 278	15.517 04	15.519 94	15.516 68	15.480 08	15.474 87	15.491 01	15.625 87	15.571 65
$(^{208}\text{Pb}/^{204}\text{Pb})_i$	37.66 050	37.863 59	37.852 12	37.851 32	37.597 60	37.636 03	37.683 07	37.741 55	37.663 80

注:误差为 2σ 。同位素校正公式: $(^{87}\text{Sr}/^{86}\text{Sr})_i = (^{87}\text{Sr}/^{86}\text{Sr})_{\text{样品}} + (^{87}\text{Rb}/^{86}\text{Sr})(e^{\lambda t} - 1)$, $\lambda_{\text{Rb}} = 1.42 \times 10^{-11} \text{ a}^{-1}$; $\epsilon_{\text{Nd}}(t) = [(^{143}\text{Nd}/^{144}\text{Nd})_{\text{样品}} / (^{143}\text{Nd}/^{144}\text{Nd})_{\text{CHUR}(t)} - 1] \times 10^4$, $(^{143}\text{Nd}/^{144}\text{Nd})_{\text{CHUR}(t)} = 0.512 638 - 0.196 7 \times (e^{\lambda t} - 1)$, $\lambda_{\text{Sm}} = 6.54 \times 10^{-12} \text{ a}^{-1}$; 亏损地幔的 Sm-Nd 同位素组成采用 $(^{143}\text{Nd}/^{144}\text{Nd})_{\text{CHUR}(t)} = 0.513 15$, $(^{147}\text{Sm}/^{144}\text{Nd})_{\text{CHUR}} = 0.213 7$ 。

5 讨论

5.1 双峰式火山岩成因

火山岩的基性端元具有两组 $^{87}\text{Sr}/^{86}\text{Sr}$ 初始值 (0.703 3~0.704 0 和 0.705 0~0.705 5) 和一致的

$\epsilon_{\text{Nd}}(t)$, 显示出地壳混染的信息。同时,基性端元具有低的 $\text{Mg}^\#$ 和 Cr 及 Ni 含量,说明它们并不是原始岩浆,而是经过了分离结晶作用形成的岩浆。 SiO_2 与 MgO 、 TiO_2 、 TFeO 、 CaO 、Cr、Ni 的负相关关系(图 9),可能指示了橄榄石及单斜辉石的分离结晶作用。

基性端元与酸性端元 SiO_2 成分存在明显的间

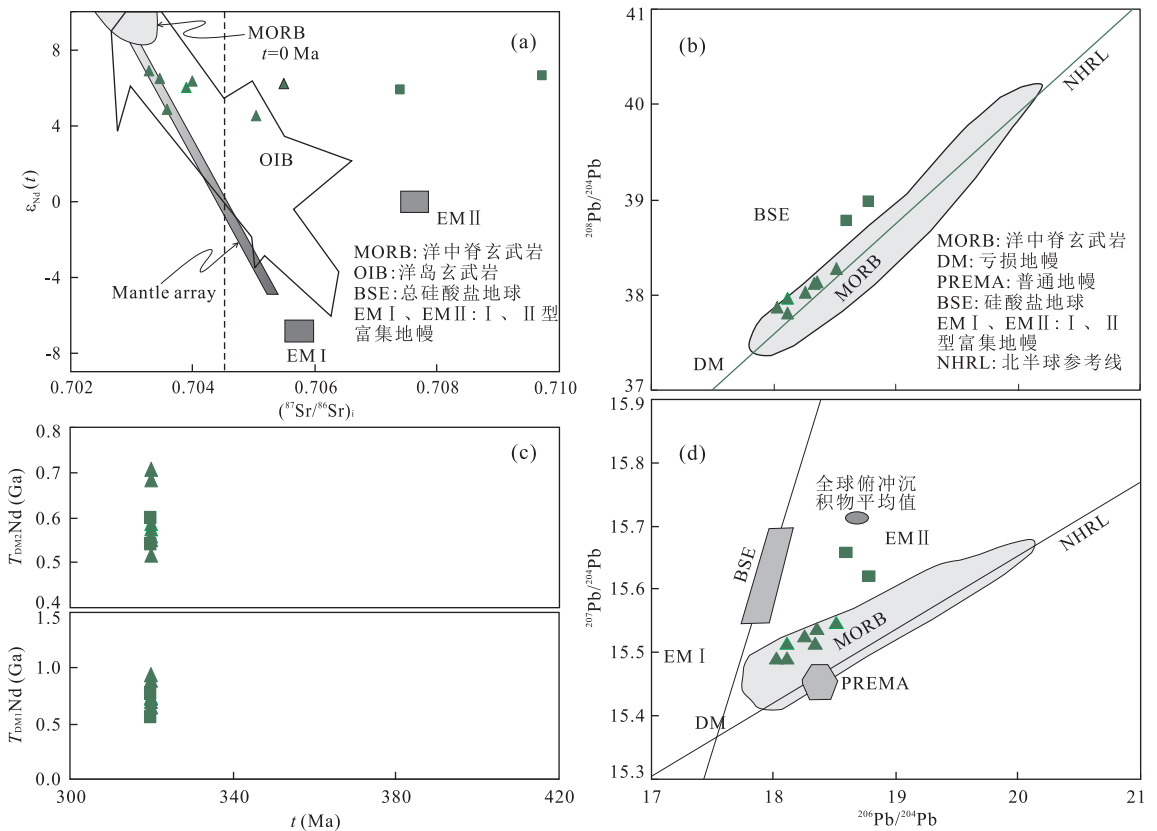


图 8 东准噶尔卡拉麦里地区巴塔玛依内山组双峰式火山岩初始 Sr-Nd-Pb 图

Fig.8 Initial Sr-Nd-Pb isotope data for the volcanic rocks from Late Carboniferous Batamayineishan Formation, eastern Junggar a. $(^{87}\text{Sr}/^{86}\text{Sr})_i - \epsilon_{\text{Nd}}(t)$ 图解 (MORB、OIB、EM I 和 EM2 据 Zimmer *et al.*, 1995); b 和 d. $^{208}\text{Pb}/^{204}\text{Pb} - ^{206}\text{Pb}/^{204}\text{Pb}$ 和 $^{207}\text{Pb}/^{204}\text{Pb} - ^{206}\text{Pb}/^{204}\text{Pb}$ 图解 (DMM、EM I 和 EMII 据 Zindler and Hart, 1986; MORB 和 NHRL 据 White *et al.*, 1987); c. $T_{\text{DM2}}\text{Nd}-t$ 和 $T_{\text{DM1}}\text{Nd}-t$ 图解; 图例同图 5

断,基性岩贫 K,酸性岩富 K,不一致的微量元素配分曲线可能指示了二者来自于不同的岩浆源区.在 Sr-Nd-Pb 同位素特征上,明显不同的 $^{87}\text{Sr}/^{86}\text{Sr}$ 初始值及 $^{206}\text{Pb}/^{204}\text{Pb}$ 、 $^{207}\text{Pb}/^{204}\text{Pb}$ 和 $^{208}\text{Pb}/^{204}\text{Pb}$ 比值也支持该套双峰式火山岩并非来自于同一源区.在 Th/Yb-Ta/Yb 图解 (Pearce *et al.*, 1990) 中,基性端元火山岩显示为 MORB 的源区属性,而在图 10a 和 10b 中,显示 MORB 的源区属性并带有弧火山岩特点.同时, Sr-Nd-Pb 同位素特征也显示了亏损的地幔源区特点.酸性端元火山岩具有与基性端元火山岩明显不同的 $^{87}\text{Sr}/^{86}\text{Sr}$ 初始值和 Pb 同位素组成,但具有相似的 $\epsilon_{\text{Nd}}(t)$ 值.关于双峰式火山岩套中的酸性端元的岩石成因目前有两种普遍的认识:(1)由基性端元火山岩直接分离结晶而来 (Turner *et al.*, 1992; Mungall and Martin, 1995; Civetta *et al.*, 1998; Ngounounoa *et al.*, 2000; Shinjo and Kato, 2000; Peccerillo *et al.*, 2003; Tian *et al.*, 2010), 这种情况下,基性端元与酸性端元火山岩来自于相同的母岩浆并显示出相似的微量元素特征和同位素特征;(2)底侵作用导致下部地壳

的部分熔融作用 (MacDonald *et al.*, 1987; Davies and Macdonald, 1987; Sage *et al.*, 1996; Trua *et al.*, 1998; Pamić *et al.*, 2000; Wareham *et al.*, 2001; Van Wagoner *et al.*, 2002; Brewer *et al.*, 2004). 这种情况下基性端元与酸性端元岩石显示出明显不同的微量元素和 Sr-Nd-Pb 同位素特征.考虑到不同的 Sr-Nd-Pb 同位素特征与微量元素特征,笔者认为该套双峰式火山岩基性端元与酸性端元来自于不同源区,基性端元来自于地幔源区而酸性端元来自于下地壳的部分熔融.

5.2 构造意义

卡拉麦里地区晚石炭世双峰式火山岩中,基性岩由拉斑质和碱性的玄武质岩石组成,富集 LILE 和 LREE,但同时具有亏损 Nb 和 Ta 的弧火山岩特征,酸性岩具有 A 型花岗岩特征.以上地球化学特征均显示为后碰撞伸展环境下双峰式火山岩地球化学特征,例如西藏德庆地区和 Papua New Guinea 北部的 New Ireland 地区的双峰式火山岩.在图 11a 中,基性火山岩落入岛弧拉班玄武岩和 N 型洋中脊玄武岩区域,同样显示了与软流圈上涌有关的亏损

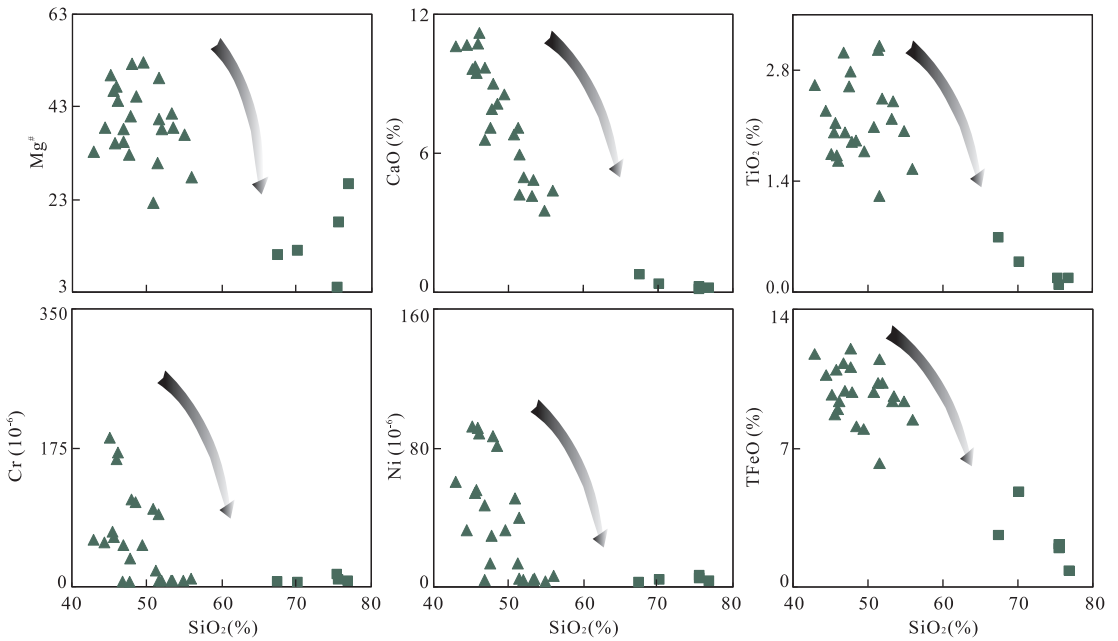


图 9 东准噶尔卡拉麦里地区巴塔玛依内山组双峰式火山岩 $Mg^\#$ 、 CaO 、 TiO_2 、 $TFeO$ 、 Cr 、 Ni 与 SiO_2 协变

Fig.9 Variations in $Mg^\#$, CaO , TiO_2 , $TFeO$, Cr , Ni , P^* and Nb^* vs. SiO_2 for the volcanic rocks from Late Carboniferous Batamayineishan Formation, eastern Junggar

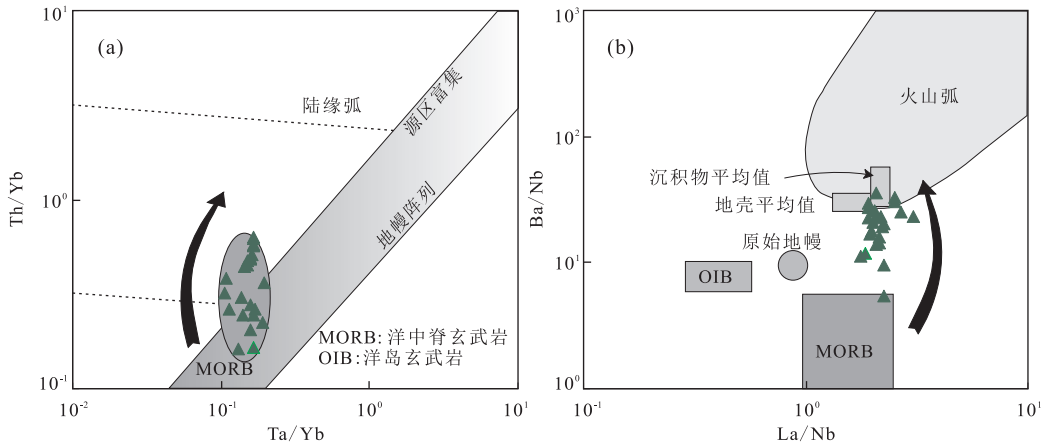


图 10 东准噶尔卡拉麦里地区巴塔玛依内山组双峰式火山岩 $Th/Yb-Ta/Yb$ 图解(a)和 $Ba/Nb-La/Nb$ 图解(b)

Fig.10 Th/Yb vs. Ta/Yb diagram (a) and Ba/Nb vs. La/Nb diagram (b) for the Middle Devonian to Late Carboniferous volcanic rocks from Batamayineishan Formation, eastern Junggar

a.据 Pearce *et al.*(1990); b.据 Jahn *et al.*(1999); MORB, OIB, 原始地幔据 Sun and McDonough(1989); 地壳平均值据 Taylor and McLennan (1985)和 Condie(1993); 沉积物平均值据 Condie(1993); 图例同图 5

地幔源区性质及弧火山岩源区特点 (Huppert and Sparks, 1988; Fountain and Christensen, 1989), 且存在由钙碱性岩浆向 N-MORB 演化的趋势, 这可能说明了该基性岩浆是在古大洋关闭的后碰撞伸展阶段所形成. 在图 11b 中, 酸性火山岩同样落入弧火山岩与板内火山岩过渡的区域, 该区域为 Pearce (1995) 补充圈定的后碰撞花岗岩叠加区域内. 在卡拉麦里断裂以北的黄羊山、老鸭泉等地, 关于后碰撞

A 型花岗岩有大量的报道 (韩宝福等, 2006; 苏玉平等, 2008; 韩宇捷等, 2012), 年龄集中在 292 ~ 311 Ma, 形成于晚石炭世—早二叠世.

从卡拉麦里造山带演化的时序上看, 笔者在原卡拉麦里蛇绿岩带南 40 km 的新疆东准噶尔卡拉麦利 1:5 万 5 幅区调 (2014) 滴水泉幅新发现的以下两点都限定了卡拉麦里洋盆的关闭时间不晚于晚泥盆世早期: (1) 418 Ma 具洋中脊特征的蛇绿混杂

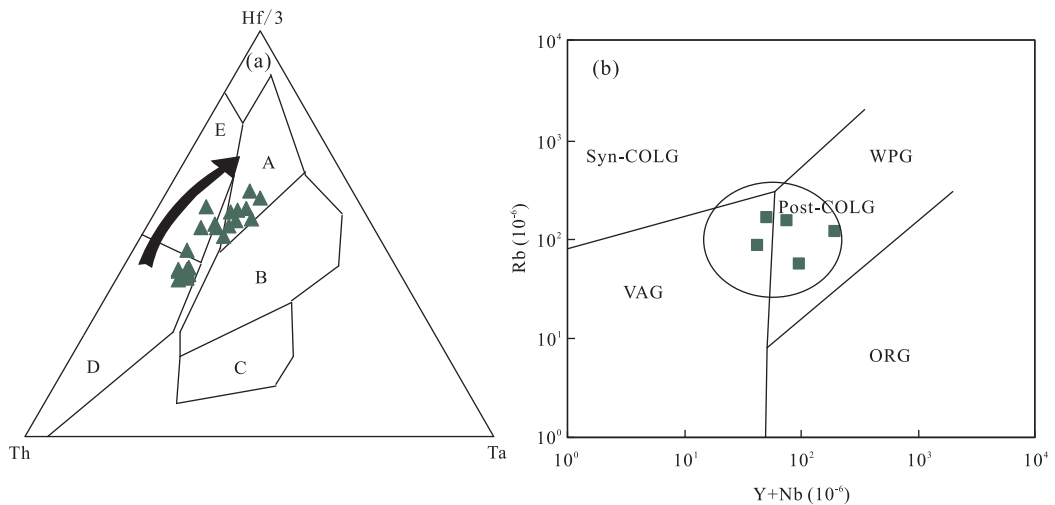


图 11 东准噶尔卡拉麦里地区巴塔玛依内山组双峰式火山岩(a)基性岩 Hf/3-Th-Ta 构造判别图解和(b)酸性岩 Rb-Y+Nb 构造判别图解

Fig.11 Tectonic discrimination diagrams of Hf/3-Th-Ta (a) and Rb vs. Y+Nb (b) for Late Carboniferous volcanic rocks from Batamayineishan Formation, eastern Junggar

a, b. 据 Pearce *et al.* (1984) 和 Pearce and Peate (1995); A. N 型大洋中脊玄武岩; B. E 型大洋中脊玄武岩和板内玄武岩; C. 板内碱性玄武岩; D. 钙碱性玄武岩; E. 岛弧拉斑玄武岩. ORG. 大洋中脊花岗岩; Syn-COLG. 同碰撞花岗岩; Post-COLG. 后碰撞; VAG. 岛弧花岗岩; WPG. 板内花岗岩; 图例同图 5

岩(胡朝斌等, 2014); (2) 早石炭世松喀尔苏组下部陆相磨拉石建造与下伏中泥盆统卡拉麦里海相堆积间的角度不整合关系(Zhang *et al.*, 2013). Zhou *et al.* (2008) 认为整个准噶尔地区石炭纪时处于后碰撞伸展背景. 区内广泛发育的早石炭世火山岩及花岗岩均具有后碰撞岩浆活动的特征(姜芸等, 2015; 田健等, 2015), 表明卡拉麦里造山带于早石炭世进入后碰撞演化阶段, 且该后碰撞过程一直持续到了晚石炭世中晚期(Chen and Arakawa, 2005; Su *et al.*, 2007; Zhang *et al.*, 2009; Su *et al.*, 2012; Xu *et al.*, 2013). 后碰撞是一个非常复杂的岩浆作用过程, 它包括了微陆块俯冲、大规模的剪切运动和连续或幕式的岩石圈扩张导致的岩石圈的拆沉与裂解(Liégeois *et al.*, 1998). 随着后碰撞阶段的演化, 在后碰撞末期由于残留洋壳的拆沉引发软流圈地幔上涌, 导致岩石圈的伸展并减薄, 从而引发双峰式火山岩岩浆作用.

综合以上信息并结合前人的研究成果, 笔者认为在 320 Ma 时, 俯冲下去的卡拉麦里洋壳发生拆离(Davies and von Blanckenburg, 1995), 引发软流圈上涌, 使得上覆的曾经被交代过的地幔发生部分熔融产生岩浆, 随后经过分离结晶作用和地壳物质的混染喷出地表形成该套双峰式火山岩的基性端元, 同时由于底侵作用导致地壳下部发生部分熔融

形成岩浆, 喷出地表形成酸性端元, 二者构成双峰式火山岩套(Davies and von Blanckenburg, 1995; Zeck, 1996; Coulon *et al.*, 2002). 该后碰撞造山阶段双峰式火山岩为造山阶段末期形成.

6 结论

(1) 卡拉麦里地区巴塔玛依内山组火山岩组合形成于晚石炭世早期 321.0 ± 4.2 Ma, 为晚石炭世早期陆相喷发的产物, 并在后期被 309.1 ± 3.0 Ma 的流纹斑岩侵入. 火山岩具明显的双峰式组合的特征, 基性端元由碱性系列和拉斑系列的玄武岩、玄武质粗面安山岩组成; 酸性端元由粗面岩和流纹岩组成, 成分上相当于 A 型花岗岩.

(2) 火山岩来源于不同的岩浆源区, 基性岩来自于亏损的地幔源区, 在岩浆上升过程中发生了橄榄石及单斜辉石的分离结晶作用并遭受了地壳混染, 而酸性岩来自于下地壳的部分熔融.

(3) 该套双峰式火山岩产出于后碰撞末期的构造环境, 由于洋壳的拆沉作用而引发软流圈上涌, 使得上覆的地幔发生部分熔融产生岩浆, 同时由于底侵作用导致地壳下部发生部分熔融, 喷出地表形成该双峰式火山岩套, 这套双峰式火山岩的出现, 标志着东准噶尔卡拉麦里地区造山作用进入尾声.

致谢:衷心感谢两位审稿人及编委对本文提出的修改建议以及地质过程与矿产资源实验室的老师在样品测试中给予的帮助!

References

- Brewer, T. S., Ahall, K. I., Menuge, J. F., et al., 2004. Mesoproterozoic Bimodal Volcanism in SW Norway, Evidence for Recurring Pre-Sveconorwegian Continental Margin Tectonism. *Precambrian Research*, 134(3-4): 249-273. doi:10.1016/j.precamres.2004.06.003
- Chen, B., Jahn, B. M., 2004. Genesis of Post-Collisional Granitoids and Basement Nature of the Junggar Terrane, NW China; Nd-Sr Isotope and Trace Element Evidence. *Journal of Asian Earth Sciences*, 23(5): 691-703. doi:10.1016/s1367-9120(03)00118-4
- Chen, B., Arakawa, Y., 2005. Elemental and Nd-Sr Isotopic Geochemistry of Granitoids from the West Junggar Foldbelt (NW China), with Implications for Phanerozoic Continental Growth. *Geochimica et Cosmochimica Acta*, 69(5): 1307-1320. doi:10.1016/j.gca.2004.09.019
- Civetta, L., D'Antonio, M., Orsi, G., et al., 1998. The Geochemistry of Volcanic Rocks from Pantelleria Island, Sicily Channel: Petrogenesis and Characteristics of the Mantle Source Region. *Journal of Petroleum*, 39(8): 1453-1491. doi:10.1093/etroj/39.8.1453
- Condie, K. C., 1993. Chemical Composition and Evolution of the Upper Continental Crust: Contrasting Results from Surface Samples and Shales. *Chemical Geology*, 104(1-4): 1-37. doi:10.1016/0009-2541(93)90140-e
- Coulon, C., Megartsi, M., Fourcade, S., et al., 2002. Post-Collisional Transition from Calc-Alkaline to Alkaline Volcanism during the Neogene in Oranie (Algeria): Magmatic Expression of a Slab Breakoff. *Lithos*, 62(3-4): 87-110. doi:10.1016/s0024-4937(02)00109-3
- Davies, G. R., Macdonald, R., 1987. Crustal Influences in the Petrogenesis of the Naivasha Basalt-Comendite Complex: Combined Trace Element and Sr-Nd-Pb Isotope Constraints. *Journal of Petroleum*, 28(6): 1009-1031. doi:10.1093/petrology/28.6.1009
- Davies, J. H., von Blanckenburg, F., 1995. Slab Break Off: A Model of Lithosphere Detachment and Its Test in the Magmatism and Deformation of Collisional Orogens. *Earth and Planetary Science Letters*, 129(1-4): 85-102. doi:10.1016/0012-821x(94)00237-s
- Donnelly, T. W., Rogers, J. J. W., 1980. Igneous Series in Island arcs: The Northeastern Caribbean Compared with Worldwide Island-Arc Assemblages. *Bulletin of Volcanology*, 43(2): 347-382. doi:10.1007/bf02598038
- Fountain, D. M., Christensen, N. I., 1989. Composition of the Continental Crust and Upper Mantle: A Review. *Memoir of the Geological Society of America*, 172: 711-742. doi:10.1130/mem172-p711
- Frisch, W., Dunkl, I., Kuhlemann J., 2000. Post-Collisional Orogen-Parallel Large-Scale Extension in the Eastern Alps. *Tectonophysics*, 327(3-4): 239-265. doi:10.1016/s0040-1951(00)00204-3
- Geist, H. L., 1995. The Generation of Oceanic Rhyolites by Crystal Fractionation: The Basalt-Rhyolite Association at Volcan Alcedo, Galapagos-Archipelago. *Journal of Petrology*, 36(4): 965-982.
- Geng, H. Y., Sun, M., Yuan, C., et al., 2009. Geochemical, Sr-Nd and Zircon U-Pb-Hf Isotopic Studies of Late Carboniferous Magmatism in the West Junggar, Xinjiang; Implications for Ridge Subduction? *Chemical Geology*, 266(3-4): 364-389. doi:10.1016/j.chemgeo.2009.07.001
- Han, B. F., Ji, J. Q., Song, B., et al., 2006. Late Paleozoic Vertical Growth of Continental Crust around the Junggar Basin, Xinjiang, China (Part I): Timing of Post-Collisional Plutonism. *Acta Petrologica Sinica*, 22(5): 1077-1086 (in Chinese with English abstract).
- Han, Y. J., Tang, H. F., Gan, L., 2012. Zircon U-Pb Ages and Geochemical Characteristics of the Laoyaquan A-Type Granites in East Junggar, North Xinjiang, China. *Acta Mineralogy Sinica*, 32(2): 193-199 (in Chinese with English abstract).
- Hochstaedter, A. G., Gill, J. B., Kusakabe, M., 2013. Volcanism in the Sumisu Rift. I. Element, Volatile and Stable Geochemistry. *Earth and Planetary Science Letters*, 100(1-3): 179-194. doi:10.1016/0012-821x(90)90184-y
- Hu, C. B., Liao, Q. A., Tian, J., et al., 2014. The Discovery and Tectonic Implication of MOR-Type Ophiolites from the Dishuiquan in Eastern Junggar. *Chinese Science Bulletin*, 59(22): 2213-2224 (in Chinese with English abstract).
- Huppert, H. E., Sparks, R. S. J., 1988. The Generation of Granitic Magmas by Intrusion of Basalt into Continental Crust. *Journal of Petrology*, 29(3): 599-624. doi:10.1093/petrology/29.3.599
- Irvine, T. N., Baragar, W. R. A., 1971. A Guide to the Chemical Classification of the Common Volcanic Rocks. *Canadian Journal of Earth Science*, 8: 523-528.
- Jahn, B. M., Wu, F., Lo, C. H., et al., 1999. Crust-Mantle Interaction Induced by Deep Subduction of the Continental Crust: Geochemical and Sr-Nd Isotopic Evidence from Post-Collisional Mafic-Ultramafic Intrusions of the Northern Dabie Complex, Central China. *Chemical*

- Geology*, 157(1–2): 119–146. doi: 10.1016/s0009–2541(98)00197–1
- Jian, P., Liu, D. Y., Zhang, Q., et al., 2003. SHRIMP Dating of Ophiolite and Leucocratic Rocks within Ophiolite. *Earth Science Frontiers*, 10(4): 439–456 (in Chinese with English abstract).
- Jiang, Y., Xiao, L., Zhou, P., et al., 2015. Geological, Geochemical Characteristics of Hongshan Pluton: Constraint for Lower Crust of West Junggar, Xinjiang. *Earth Science*, 40(7): 1129–1147 (in Chinese with English abstract).
- Liégeois, J. P., Navez, J., Hertogen, J., et al., 1998. Contrasting Origin of Post-Collisional High-K Calc-Alkaline and Shoshonitic Versus Alkaline and Peralkaline Granitoids. The Use of Sliding Normalization. *Lithos*, 45(1–4): 1–28. doi: 10.1016/s0024–4937(98)00023–1
- Li, Y. J., Yang, G. X., Wu, H. E., et al., 2009. The Determination of Beilekuduke Aluminous A-Type Granites in East Junggar, Xinjiang. *Acta Petrologica et Mineralogica*, 28(1): 17–25 (in Chinese with English abstract).
- Li, D., He, D. F., Fan, C., et al., 2012. Geochemical Characteristics and Tectonic Significance of Carboniferous Basalt in the Karamaili Gas Field of Junggar Basin. *Acta Petrologica Sinica*, 28(3): 981–992 (in Chinese with English abstract).
- Li, J. Y., Xiao, X. C., Tang, Y. Q., et al., 1990. Main Characteristics of Late Paleozoic Plate Tectonic in the Southern Part of East Junggar, Xinjiang. *Geological Review*, 36(4): 305–316 (in Chinese with English abstract).
- Liu, Y. S., Hu, Z. C., Gao, S., et al., 2008. In Situ Analysis of Major and Trace Elements of Anhydrous Minerals by LA-ICP-MS without Applying an Internal Standard. *Chemical Geology*, 257(1–2): 34–43. doi: 10.1016/j.chemgeo.2008.08.004
- Liu, Y. S., Gao, S., Hu, Z. C., et al., 2009. Continental and Oceanic Crust Recycling-Induced Melt-Peridotite Interactions in the Trans-North China Orogen: U-Pb dating, Hf Isotopes and Trace Elements in Zircons of Mantle Xenoliths. *Journal of Petrology*, 51(1–2): 537–571. doi: 10.1093/petrology/egp082
- Liu, W., Liu, X. J., Liu, L. J., et al., 2013. Underplating Generated A- and I-Type Granitoids of the East Junggar from the Lower and the Upper Oceanic Crust with Mixing of Mafic Magma: Insights from Integrated Zircon U-Pb Ages, Petrography, Geochemistry and Nd-Sr-Hf Isotopes. *Lithos*, 179: 293–319. doi: 10.1016/j.lithos.2013.08.009
- Ludwig, K. R., 2003. Users Manual for Isoplot 3.0: A Geochronological Toolkit for Microsoft Excel. Berkeley Geochronology Center, California.
- MacDonald, R., Sparks, R. S. J., Sigurdsson, H., et al., 1987. The 1875 Eruption of Askja Volcano Iceland: Combined Fractional Crystallization and Selective Contamination in the Generation of Rhyolitic Magma. *Mineralogical Magazine*, 51: 183–202.
- Mungall, J. E., Martin, R. F., 1995. Petrogenesis of Basalt-Comendite and Basalt Pantellerite Suites, Terceira, Azores, and some Implications for the Origin of Oceanic Rhyolites. *Contributions to Mineralogy and Petrology*, 119(1): 43–55. doi: 10.1007/bf00310716
- Ngounouno, I., Déruelle, B., Demaiffe, D., 2000. Petrology of the Bimodal Cenozoic Volcanism of the Kapsiki Plateau (Northernmost Cameroon, Central Africa). *Journal of Volcanology and Geothermal Research*, 102(1–2): 21–44. doi: 10.1016/s0377–0273(00)00180–3
- Pamić, J., Belak, M., Bullen, T. D., et al., 2000. Geochemistry and Geodynamics of a Late Cretaceous Bimodal Volcanic Association from the Southern Part of the Pannonian Basin in Slavonija (Northern Croatia). *Mineralogy and Petrology*, 68(4): 271–296. doi: 10.1007/s007100050013
- Pearce, J. A., Harris, N. B. W., Tindle, A. G., 1984. Trace Element Discrimination Diagrams for the Tectonic Interpretation of Granitic Rocks. *Journal of Petrology*, 25(4): 956–983. doi: 10.1093/petrology/25.4.956
- Pearce, J. A., Bender, J. F., de Long, S. E., et al., 1990. Genesis of Collision Volcanism in Eastern Anatolia Turkey. *Journal of Volcanology and Geothermal Research*, 44(1–2): 189–229. doi: 10.1016/0377–0273(90)90018–b
- Pearce, J. A., Peate, D. W., 1995. Tectonic Implications of the Composition of Volcanic Arc Magmas. *Annual Review of Earth and Planetary Sciences*, 23(1): 251–286. doi: 10.1146/annurev.ea.23.050195.001343
- Peccerillo, A., Barberio, M. R., Yirgu, G., et al., 2003. Relationship between Mafic and Peralkaline Felsic Magmatism in Continental Rift Settings: A Petrological, Geochemical and Isotopic Study of the Gedemsa Volcano, Central Ethiopian Rift. *Journal of Petroleum*, 44(11): 2003–2032. doi: 10.1093/petrology/egg068
- Peccerillo, A., Taylor, S. R., 1976. Geochemistry of Eocene Calc-Alkaline Volcanic Rocks from the Kastamonu Area, Northern Turkey. *Contributions to Mineralogy and Petrology*, 58(1): 130–143. doi: 10.1007/bf00384745
- Sage, R. P., Lightfoot, P. C., Doherty, W., 1996. Bimodal Cyclical Archean Basalts and Rhyolites from the Michipicoten (Wawa) Greenstone Belt, Ontario: Geochemical Ev-

- idence for Magma Contributions from the Asthenospheric Mantle and Ancient Continental Lithosphere near the Southern Margin of the Superior Province. *Precambrian Research*, 76(3-4): 119-153. doi: 10.1016/0301-9268(95)00020-8
- Shinjo, R., Kato, Y., 2000. Geochemical Constraints on the Origin of Bimodal Magmatism at the Okinawa Trough, an Incipient Back-Arc Basin. *Lithos*, 54(3-4), 117-137. doi: 10.1016/s0024-4937(00)00034-7
- Sun, S. S., McDonough, W. F., 1989. Chemical and Isotopic Systematics of Oceanic Basalts: Implications for Mantle Composition and Processes. *Geological Society London Special Publications*, 42(1): 313-345. doi: 10.1144/gsl.sp.1989.042.01.19
- Su, Y. P., Tang, H. F., Cong, F., et al., 2008. Zircon U-Pb Age and Petrogenesis of the Huangyangshan Alkal Negrinite Body in East Junggar Xinjiang. *Acta Mineralogy Sinica*, 28(2): 117-126 (in Chinese with English abstract).
- Su, Y. P., Tang, H. F., Liu, C. Q., et al., 2006. The Determination and a Preliminary Study of Sujiquan Aluminous a Type Granites in East Junggar, Xinjiang. *Acta Petrologica et Mineralogica*, 25(3): 175-184 (in Chinese with English abstract).
- Su, Y. P., Zheng, J. P., Griffin W. L., et al., 2010. Zircon U-Pb and Hf Isotopes of Volcanic Rocks from the Batamayneishan Formation in the Eastern Junggar Basin. *Chinese Science Bulletin*, 55(30): 2931-2943 (in Chinese with English abstract).
- Su, Y. P., Tang, H. F., Sylvester, P. J., et al., 2007. Petrogenesis of Karamaili Alkaline A-Type Granites from East Junggar, Xinjiang (NW China) and Their Relationship with Tin Mineralization. *Geochemical Journal*, 41(5): 341-357. doi: 10.2343/geochemj.41.341
- Su, Y. P., Zheng, J. P., Griffin, W. L., et al., 2012. Geochemistry and Geochronology of Carboniferous Volcanic Rocks in the Eastern Junggar Terrane, NW China: Implication for a Tectonic Transition. *Gondwana Research*, 22(3-4): 1009-1029. doi: 10.1016/j.gr.2012.01.004
- Taylor, S. R., McLennan, S. M., 1985. *The Continental Crust, Its Composition and Evolution*. Blackwell, Oxford.
- Tan, J. Y., Wu, R. J., Zhang, Y. Y., et al., 2009. Characteristics and Geochronology of Volcanic Rocks of Batamayneishan Formation in Kalamaili, Eastern Junggar, Xinjiang. *Acta Petrologica Sinica*, 25(3): 539-546 (in Chinese with English abstract).
- Tang, H. F., Su, Y. P., Liu, C. Q., et al., 2007. Zircon U-Pb Age of the Plagiogranite in Kalamaili Belt, Northern Xinjiang and Its Tectonic Implications. *Geotectonica et Metallogenia*, 31(1): 110-117 (in Chinese with English abstract).
- Tian, W., Campbell, I. H., Allen, C. M., et al., 2010. The Tarim Picrite-Basalt-Rhyolite Suite, a Permian Flood Basalt from Northwest China with Contrasting Rhyolites Produced by Fractional Crystallization and Anatexis. *Contributions to Mineralogy and Petrology*, 160(3): 407-425. doi: 10.1007/s00410-009-0485-3
- Tian, J., Liao, Q. A., Fan, G. M., et al., 2015. The Discovery and Tectonic Implication of Early Carboniferous Post-Collisional I-Type Granites from the South of Karamaili in Eastern Junggar. *Acta Petrologica Sinica*, 31(5): 1471-1484 (in Chinese with English abstract).
- Trua, T., Deniel, C., Mazzuoli, R., 1998. Crustal Control in the Genesis of Plio-Quaternary Bimodal Magmatism of the Main Ethiopian Rift (MER): Geochemical and Isotopic Evidence. *Chemical Geology*, 155(3-4): 201-231. doi: 10.1016/s0009-2541(98)00174-0
- Turner, S. P., Foden, J. D., Morrison, R. S., 1992. Derivation of Some A-Type Magmas by Fractionation of Basaltic Magma: An Example from the Padthaway Ridge, South Australia. *Lithos*, 28(2): 151-179. doi: 10.1016/0024-4937(92)90029-x
- van Wagoner, N. A., Leybourne, M. I., Dadd, K. A., et al., 2002. Late Silurian Bimodal Volcanism of Southwestern New Brunswick, Canada: Products of Continental Extension. *Geological Society of America Bulletin*, 114(4): 400-418. doi: 10.1130/0016-7606(2002)114<0400:lsbvos>2.0.co;2
- Vavra, G., Schmid, R., Gebauer, D., 1999. Internal Morphology, Habit and U-Th-Pb Microanalysis of Amphibolite-to-Granulite Facies Zircons: Geochronology of the Ivrea Zone (Southern Alps). *Contributions to Mineralogy and Petrology*, 134(4): 380-404. doi: 10.1007/s004100050492
- Wang, F. M., Liao, Q. A., Fan, G. M., et al., 2014. Geological Implications of Unconformity between Upper and Middle Devonian, and 346.8 Ma Post-Collision Volcanic Rocks in Karamaili, Xinjiang. *Earth Science*, 39(9): 1243-1257 (in Chinese with English abstract).
- Wang, J. B., Xu, X., 2006. Post-Collisional Tectonic Evolution and Metallogensis in Northern Xinjiang, China. *Acta Geologica Sinica*, 80(1): 23-31 (in Chinese with English abstract).
- Wareham, C. D., Stump, E., Storey, B. C., et al., 2001. Petrogenesis of the Cambrian Liv Group, a Bimodal Volcanic Rock Suite from the Ross Orogen, Transantarctic Mountains. *Geological Society of America Bulletin*,

- 113(3):360—372. doi:10.1130/0016-7606(2001)113<0360:potclg>2.0.co;2
- White, W.M., Hofmann, A.W., Puchel, H., 1987. Isotopic Geochemistry of Pacific Midocean Ridge Basalt. *Journal of Geophysics Research*, 92:4881—4893.
- Wu, R.J., Zhang, Y.Y., Tan, J.Y., et al. 2009. The Characteristics of Different Structure Layers and Tectonic Implications since Late Paleozoic in Kalamaily Area, Xinjiang. *Earth Science Frontiers*, 16(3):102—109 (in Chinese with English abstract).
- Xiao, W.J., 2008. Middle Cambrian to Permian Subduction-Related Accretionary Orogenesis of Northern Xinjiang, NW China; Implications for the Tectonic Evolution of Central Asia. *Journal of Asian Earth Sciences*, 32(2—4):102—177. doi:10.1016/j.jseas.2007.10.008
- Xiao, W., Huang, B., Han, C., et al., 2010. A Review of the Western Part of the Altaids: A Key to Understanding the Architecture of Accretionary Orogens. *Gondwana Research*, 18:253—273.
- Xu, X.W., Jiang, N., Li, X.H., et al., 2013. Tectonic Evolution of the East Junggar Terrane: Evidence from the Taheir Tectonic Window, Xinjiang, China. *Gondwana Research*, 24(2):578—600. doi:10.1016/j.gr.2012.11.007
- Zhang, Y., Pe-Piper, G., Piper, D.J., 2013. Early Carboniferous Collision of the Kalamaili Orogenic Belt, North Xinjiang, and Its Implications: Evidence from Molasse Deposits. *Geological Society of America Bulletin*, 125(5—6):932—944. doi:10.1130/b30779.1
- Zhang, Z.C., Zhou, G., Kusky, T.M., et al., 2009. Late Paleozoic Volcanic Record of the Eastern Junggar Terrane, Xinjiang, Northwestern China: Major and Trace Element Characteristics, Sr-Nd Isotopic Systematics and Implications for Tectonic Evolution. *Gondwana Research*, 16(2):201—215. doi:10.1016/j.gr.2009.03.004
- Zhang, Y.Y., Chen, S., Guo, Z.J., et al., 2009. Zircon SHRIMP U-Pb Dating of the Latest Paleozoic Volcanic Rocks in Zhabahe Area, Eastern Junggar and Its Geological Implications. *Acta Petrologica Sinica*, 25(3):506—514 (in Chinese with English abstract).
- Zeck, H.P., 1996. Betic-Rif Orogeny: Subduction of Mesozoic Tethys Lithosphere under Eastward Drifting Iberia, Slab Detachment Shortly before 22 Ma, and Subsequent Uplift and Extensional Tectonics. *Tectonophysics*, 254(1—2):1—16. doi:10.1016/0040-1951(95)00206-5
- Zhou, T.F., Yuan, F., Fan, Y., et al., 2008. Granites in the Sawuer Region of the West Junggar, Xinjiang Province, China: Geochronological and Geochemical Characteristics and Their Geodynamic Significance. *Lithos*, 106(3—4):191—206. doi:10.1016/j.lithos.2008.06.014
- Zhu, Z.X., Li, S.Z., Li, S.L., 2005. The Characteristics of Sedimentary System-Continental Facies Volcano in Later Carboniferous Batamayineishan Group, Zhifang Region, East Junggar. *Xinjiang Geology*, 23(1):14—18 (in Chinese with English abstract).
- Zimmer, M., Kroner, A., Jochum, K. P., et al., 1995. The Gabal Gerf Complex: A Precambrian N-MORB Ophiolite in the Nubian Shield, NE Africa. *Chemical Geology*, 123:29—51.
- Zindler, A., Hart, S.R., 1986. Chemical Geodynamics. *Annual Review of Earth Planetary Sciences*, 14:493—571.

附中 文 参 考 文 献

- 韩宝福, 季建清, 宋彪, 等, 2006. 新疆准噶尔晚古生代陆壳垂向生长(I)——后碰撞深成岩浆活动的时限. *岩石学报*, 22(5):1077—1086.
- 韩宇捷, 唐红峰, 甘林, 2012. 新疆东准噶尔老鸦泉岩体的锆石 U-Pb 年龄和地球化学组成. *矿物学报*, 32(2):193—199.
- 胡朝斌, 廖群安, 樊光明, 等, 2014. 东准噶尔滴水泉地区发现洋中脊型蛇绿岩. *科学通报*, 59(22):2213—2224.
- 简平, 刘敦一, 张旗, 等, 2003. 蛇绿岩及蛇绿岩中浅色岩的 SHRIMP U-Pb 测年. *地学前缘*, 59(22):439—456.
- 姜芸, 肖龙, 周佩, 等, 2015. 新疆西准噶尔红山岩体地质地球化学特征及对下地壳性质的启示. *地球科学*, 40(7):1129—1147.
- 李永军, 杨高学, 吴宏恩, 等, 2009. 东准噶尔贝勒库都克铝质 A 型花岗岩的厘定及意义. *岩石矿物学杂志*, 28(1):17—25.
- 李涤, 何登发, 樊春, 等, 2012. 准噶尔盆地克拉美丽气田石炭系玄武岩的地球化学特征及构造意义. *岩石学报*, 28(3):981—992.
- 李锦铭, 肖序常, 汤耀庆, 等, 1990. 新疆东准噶尔卡拉麦里地区晚古生代板块构造的基本特征. *地质论评*, 36(4):305—316.
- 苏玉平, 唐红峰, 丛峰, 2008. 新疆东准噶尔黄羊山碱性花岗岩体的锆石 U-Pb 年龄和岩石成因. *矿物学报*, 28(2):117—126.
- 苏玉平, 唐红峰, 刘丛强, 等, 2006. 新疆东准噶尔苏吉泉铝质 A 型花岗岩的确立及其初步研究. *岩石矿物学杂志*, 25(3):175—184.
- 苏玉平, 郑建平, Griffin, W.L., 等, 2010. 东准噶尔盆地巴塔玛依内山组火山岩锆石 U-Pb 年代及 Hf 同位素研究. *科学通报*, 55(30):2931—2943.
- 谭佳奕, 吴润江, 张元元, 等, 2009. 东准噶尔卡拉麦里地区巴塔玛依内山组火山岩特征和年代确定. *岩石学报*, 25(3):539—546.

唐红峰,苏玉平,刘丛强,等,2007.新疆北部卡拉麦里斜长花岗岩的锆石 U-Pb 年龄及其构造意义.大地构造与成矿学,31(1):110-117.

田健,廖群安,樊光明,等,2015.东准噶尔卡拉麦里断裂以南早石炭世后碰撞花岗岩的发现及其地质意义.岩石学报,31(5):1471-1484.

王富民,廖群安,樊光明,等,2014.新疆卡拉麦里上一中泥盆统间角度不整合和 346.8 Ma 后碰撞火山岩的意义.地球科学,39(9):1243-1257.

王京彬,徐新,2006.新疆北部后碰撞构造演化与成矿.地质学

报,80(1):23-31.

吴润江,张元元,谭佳奕,等,2009.新疆卡拉麦里地区晚古生代以来不同构造层特征及大地构造意义.地质前缘,16(3):102-109.

张元元,陈石,郭召杰,等,2009.东准噶尔扎河坝地区古生代晚期火山岩的锆石 SHRIMP U-Pb 定年及其地质意义.岩石学报,25(3):506-514.

朱志新,李少贞,李嵩龄,2005.东准噶尔纸房地区晚石炭世巴塔玛依内山组陆相火山-沉积体系特征.新疆地质,23(1):14-18.

《地球科学》

2016 年 12 月 第 41 卷 第 12 期 要目预告

浙江省泥石流灾害发育分布规律及区域预报	冯杭建等
水化学温度计估算粤西沿海深部地热系统热交换温度	郭 静等
塔中地区深层低丰度碳酸盐岩有效烃源岩评价及其对油气藏贡献	霍志鹏等
内蒙古巴林右旗胡都格绍荣岩体的年代学、地球化学、Hf 同位素特征及构造背景	李鹏川等
内蒙古乌拉特中旗哈达呼舒基性岩体形成的构造背景与古亚洲洋的早期俯冲历史	刘金龙等
普光地区碳酸盐岩储层孔隙类型测井识别及孔渗关系	张 翔等
黔东松桃地区南华系大塘坡组锰矿中黄铁矿硫同位素特征及其地质意义	王 萍等